# Analysis of the transient thermal field in two conductors carrying sinusoidal current using Green's function

## MAREK ZARĘBA®

Bialystok University of Technology, Faculty of Electrical Engineering Department of Electrotechnics, Power Electronics and Electrical Power Engineering 45D Wiejska Str., 15-351 Białystok, Poland e-mail:m.zareba@pb.edu.pl

**Abstract:** This paper analyzes the transient thermal field in a system of two parallel conductors. The skin and proximity effects are taken into account. An analytical method based on Green's function is developed to determine the field distributions. The Green's function was determined analytically, and due to the complex forms of the expressions describing the current densities, the integrals resulting from the Green's identity were calculated numerically. In addition, important parameters determining the dynamics of the conductors were also calculated: heating curves and thermal time constants. The influence of selected material parameters on the corresponding thermal field distributions is examined. The calculation results are positively verified using the finite element method.

Key words: analytical method, heating of the wires, transient temperature state

## 1. Introduction

The analysis of thermal fields in electrical conductors and wires typically focuses on steady-state conditions, which are crucial to determining critical parameters such as the steady-state current rating [1, 2]. Transient temperature fields are studied much less frequently. However, they allow for the determination of the dynamic properties of conductors and wires, for instance, under power-on conditions, load changes, or short circuits. Knowledge of transient temperature distributions is also essential when analyzing intermittent or periodic operation [3, 4], where a conductor may be overloaded with a current exceeding the steady-state current rating.

Transient thermal fields in wires and cables can be calculated using analytical methods, numerical methods, their combinations, or methods based on thermoelectric analogy. Among these, the numerical methods [5–9] are the most widely used. They enable the analysis of systems with complex geometries and take into account the heterogeneity and non-linearity of materials.

The finite element method (FEM) [5–7] dominates among the numerical methods, while the finite difference method (FDM) [8, 9] is used less frequently. Another important group are methods based on thermoelectric analogy [10–13]. In this approach, different layers of the wire or cable are modeled using lumped like RC elements.

The last group of the aforementioned methods for calculating the unsteady thermal field in conductors and wires consists of analytical methods. These methods mainly focus on solving the partial heat conduction equation with appropriate boundary and initial conditions. Their main advantage is the possibility of obtaining solutions in the form of analytical expressions, enabling the determination of the field distribution at any point in the model. Additionally, they facilitate the physical interpretation of results, the analysis of the influence of the parameters, and the derivation of approximation and asymptotic dependencies [14, 15]. Analytical methods have been used in transient state calculations in several studies [16-19]. In [16], an unsteady onedimensional thermal field was determined in a cylindrical wire, taking into account the skin effect. The variable separation method was used to solve the appropriate mathematical model. In [17], the unsteady thermal field was determined in a tubular busbar, taking into account its variable resistivity with temperature. In this case, Green's function was used for the calculations. In turn, in [18] the unsteady thermal field was determined in the ACCR line, taking into account the influence of the wind, using the method of separation of variables for calculations. In these studies [16–18], a convective heat exchange with the surrounding environment was assumed on the external surface of the model (third-kind boundary condition). In turn, in [19] the unsteady thermal field in the cable was determined by assuming an adiabatic boundary condition (i.e., no heat exchange on the external surface). This solution is correct for relatively short time intervals. In [19], the variable separation method was used for the calculations.

The purpose of this article is to determine the unsteady thermal field in a system of two parallel conductors placed close to each other, taking into account both the skin and proximity effects [20–22]. Furthermore, in addition to determining the field distributions, other important transient parameters, such as heating curves and thermal time constants, were also determined. For this purpose, an analytical method based on the Green's function was developed. The Green's functions were determined analytically, and due to the complex forms of the expressions describing the current densities, the integrals resulting from the Green's identity were calculated numerically.

# 2. Mathematical model of the system

The subject of the analysis is a system of two parallel conductors placed close to each other (Fig. 1), separated by a distance d. It is assumed that both conductors have identical radii and that their length is much greater than the transverse dimension, defined as the sum of twice the diameter of the conductors and the distance between them. The system is assumed to be at ambient temperature  $T_0$  and shielded from direct sunlight. The thermal field in the conductors is generated by the flow of alternating current from the time t = 0 with the root-mean-square (RMS)

values of  $I_1$  and  $I_2$ , in the left and right conductors, respectively (Fig. 1). It is assumed that the conductors are placed relatively close to each other so that the electromagnetic field of one conductor penetrates the other and vice versa, inducing eddy currents in the conductors (proximity effect). With the above assumptions, the transient thermal field in the conductors will depend on time and, in the cylindrical coordinate system adopted in the following, on two geometric coordinates (r - radial coordinate, and  $\varphi$  - angular coordinate).

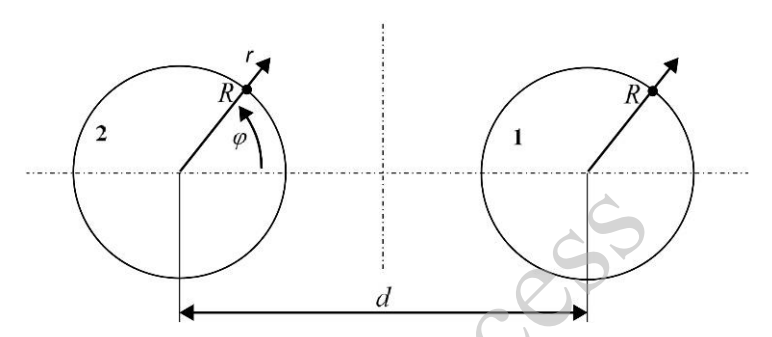


Fig. 1. A system of two identical conductors placed parallel to one other

To facilitate the solution of the mathematical model defined below, the temperature increase relative to the ambient temperature  $T_0$  is defined as follows:

$$v_i(r, \phi, t) = T_i(r, \phi, t) - T_0,$$
 (1)

where  $v_i(r, \varphi, t)$  denotes the temperature increase,  $T_0$  is the ambient temperature, i is the conductor index and t is the time.

The non-stationary temperature increase, considering the previously stated assumptions, is described by the two-dimensional heat conduction equation [23, 24] of the following form:

$$\frac{\partial^{2} v_{i}(r,\phi,t)}{\partial r^{2}} + \frac{1}{r} \frac{\partial v_{i}(r,\phi,t)}{\partial r} + \frac{1}{r^{2}} \frac{\partial v_{i}^{2}(r,\phi,t)}{\partial \phi^{2}} - \frac{1}{\chi} \frac{\partial v_{i}(r,\phi,t)}{\partial t} = -\frac{g_{i}(r,\phi)}{\lambda},$$

$$\text{for } 0 \le r \le R, \quad 0 \le \varphi \le 2\pi, \quad t > 0, \quad i = 1, 2,$$

where:  $\chi = \lambda/c\delta$ ,  $\lambda$  is the thermal conductivity of the conductor, c is the specific heat,  $\delta$  is the density. The heat source term  $g_i(r,\varphi)$  in Eq. (2) depends on the current density in the conductors and is defined as follows:

$$g_i(r,\phi) = \frac{|J_i(r,\phi)|^2}{\gamma},\tag{3}$$

where  $\gamma$  is the electrical conductivity of the conductor.

The current densities  $J_i(r,\varphi)$  in Eq. (3) include both the component resulting from the skin effect and proximity effect. The following analysis uses the results from [25], which provide approximate expressions for current densities in a system of two parallel conductors, as shown in Fig. 1:

$$J_1(r,\phi) = \frac{I_1}{\pi R^2} \frac{\Gamma R}{2} \frac{I_0(\Gamma r)}{I_1(\Gamma R)} \mp \frac{I_2}{\pi R^2} \Gamma R \sum_{n=1}^{\infty} (-1)^n \left(\frac{R}{d}\right)^n \frac{I_n(\Gamma r)}{I_{n-1}(\Gamma R)} \cos(n\phi), \tag{4}$$

for 
$$0 \le r \le R$$
,  $0 \le \varphi \le 2\pi$ ,

$$J_{2}(r,\phi) = \pm \frac{I_{2}}{\pi R^{2}} \frac{\Gamma R}{2} \frac{I_{0}(\Gamma r)}{I_{1}(\Gamma R)} \pm \frac{I_{1}}{\pi R^{2}} \Gamma R \sum_{n=1}^{\infty} \left(\frac{R}{d}\right)^{n} \frac{I_{n}(\Gamma r)}{I_{n-1}(\Gamma R)} \cos(n \phi),$$
for  $0 \le r \le R$ ,  $0 \le \varphi \le 2\pi$ ,

where  $\Gamma = \sqrt{j2\pi f \mu_0 \gamma}$ ,  $\mu_0$  is the magnetic permeability,  $j = \sqrt{-1}$  is the imaginary unit, f is the frequency. The upper and lower signs in Eqs. (4) and (5) correspond to the same and opposite directions of current flow, respectively. The functions  $I_n(...)$  are the modified Bessel functions of order n. The first terms in Eqs. (4) and (5) describe the current densities resulting from the skin effect, while the second terms, expressed as series, correspond to the proximity effect components. These expressions were derived in [25] based on the solution of Helmholtz's equation [26], using Maxwell's classical equations and the magnetic vector potential.

The described mathematical model of the thermal field is supplemented with boundary and initial conditions. It is assumed that the external surfaces of the conductors dissipate heat to the surroundings according to Newton's law [23, 24]. This is expressed by the Hankel boundary condition:

$$\frac{\partial v_i(r,\phi,t)}{\partial r}\Big|_{r=R} = -\frac{h}{\lambda} \cdot v_i(R,\phi,t),$$
for  $0 \le \varphi \le 2\pi$ ,  $t > 0$ ,  $i = 1, 2$ ,

where h is the heat transfer coefficient.

As previously assumed, the system of conductors is heated by current starting from time t = 0. This results in zero initial conditions with respect to the temperature increase.

$$v_i(r, \phi, t = 0) = 0,$$
 (7)  
for  $0 \le r \le R$ ,  $0 \le \varphi \le 2\pi$ ,  $i = 1, 2$ .

Equations (1)–(7) presented above form the mathematical model of the thermal field.

### 3. Green's function

The mathematical model (1)–(7) defined in the previous section was solved using the Green's function [27, 28]. The main advantage of the Green's function is that it does not depend on forcing (heat sources). Additionally, compared to the frequently used state superposition method [23], it is not necessary to determine the steady and transient components separately. Moreover, the solutions obtained using the Green's function are in integral form and are usually characterized by high convergence. In the analyzed system (for a single conductor), the boundary-initial problem for Green's function ( $G = G(r, \varphi, t; \rho, \theta, \eta)$ ) is formulated as follows:

$$\frac{\partial^2 G}{\partial r^2} + \frac{1}{r} \frac{\partial G}{\partial r} + \frac{1}{r^2} \frac{\partial G^2}{\partial \phi^2} - \frac{1}{r} \frac{\partial G}{\partial t} = -\frac{1}{r} \delta(r - \rho)(\phi - \theta)(t - \eta), \tag{8}$$

for 
$$0 \le r, \rho \le R$$
,  $0 \le \varphi, \theta \le 2\pi$ ,  $t \ge \eta$ ,

$$\left. \frac{\partial G}{\partial r} \right|_{r=R} = -\frac{h}{\lambda} [G]|_{r=R},\tag{9}$$

for 
$$0 \le \varphi, \theta \le 2\pi$$
,  $t \ge \eta$ ,

$$G = 0 \quad \text{for} \quad t < \eta, \tag{10}$$

$$G(r, \phi, t; \rho, \theta, \eta) = G(\rho, \theta, -\eta; r, \phi, -t), \tag{11}$$

where the right-hand side of Eq. (8) is the product of the shifted Dirac impulses (in space with respect to  $\rho$ ,  $\theta$  and in time with respect to t). In the considered system, the unsteady temperature increase, using the Green's function can be expressed by the following integral relation:

$$v_{i}(r,\phi,t) = \frac{\chi}{\lambda} \int_{0}^{R} \int_{0}^{2\pi} \int_{0}^{t} g_{i}(\rho,\theta) G(r,\phi,t;\rho,\theta,\eta) \rho d\rho d\theta d\eta,$$
for  $0 \le r \le R$ ,  $0 \le \varphi \le 2\pi$ ,  $t > 0$ ,  $i = 1, 2$ ,

where  $g_i(\rho,\theta)$  is described by the relationship (3) (after replacing  $\rho \to r$ ,  $\theta \to \varphi$ ). The integral relation (12) given above results from the application of the second Green's identity to the corresponding components of the previously defined problems (1)–(7) and (8)–(11) as well as the use of the properties of the Green's function and Dirac's delta. The condition for determining the solution based on (12) is knowledge of the Green's function G(...). To obtain it, a method of solving two simpler (e.g., homogeneous) problems can be used [28], in which one of them was solved using the Green's function. Then, by utilizing an appropriate comparison, it is possible to determine the Green's function. For this purpose, a homogeneous problem for the function  $\Theta(r,\varphi,t)$  is defined below and then solved using two methods.

$$\frac{\partial^2 \Theta(r,\phi,t)}{\partial r^2} + \frac{1}{r} \frac{\partial \Theta(r,\phi,t)}{\partial r} + \frac{1}{r^2} \frac{\partial \Theta^2(r,\phi,t)}{\partial \phi^2} - \frac{1}{\chi} \frac{\partial \Theta(r,\phi,t)}{\partial t} = 0, \tag{13}$$

for 
$$0 \le r \le R$$
,  $0 \le \varphi \le 2\pi$ ,  $t > 0$ ,

$$\frac{\partial \Theta(r,\phi,t)}{\partial r}\Big|_{r=R} = -\frac{h}{\lambda}\Theta(R,\phi,t),$$
 (14)

for 
$$0 \le \varphi \le 2\pi$$
,  $t > 0$ ,

$$\Theta(r, \varphi, t = 0) = F(r, \varphi) \quad \text{for } 0 \le r \le R, \quad 0 \le \varphi \le 2\pi, \tag{15}$$

where  $F(r, \varphi)$  is an arbitrary distribution of the initial condition.

In the first step, the problem (13)–(15) was solved using the method of separation of variables [23, 24]. By applying this method and eliminating non-physical solutions, the general solution to (13)–(15) was obtained in the form:

$$\Theta(r,\phi,t) = \sum_{m=0}^{\infty} \sum_{n=1}^{\infty} J_m \left( \alpha_{mn} \frac{r}{R} \right) \cdot \left( B_{mn} \cos(m\phi) + C_{mn} \sin(m\phi) \right) e^{-\alpha_{mn}^2 \frac{\chi}{R^2} t},$$
for  $0 \le r \le R$ ,  $0 \le \varphi \le 2\pi$ ,  $t > 0$ ,

where  $J_m(...)$  are Bessel functions of the first kind of order m,  $B_{mn}$ ,  $C_{mn}$  are unknown coefficients and  $\alpha_{mn}$  are eigenvalues. Subsequently, the eigenvalues  $\alpha_{mn}$  were determined from the eigenvalue equation, which was obtained by substituting (16) into the boundary condition (14).

$$J_{m+1}(\alpha_{mn}) - \frac{m}{\alpha_{mn}} J_m(\alpha_{mn}) - \frac{Rh}{\alpha_{mn}\lambda} J_m(\alpha_{mn}) = 0, \tag{17}$$

where  $\alpha_{mn}$  is numerically computed from Eq. (17) above.

The unknown coefficients  $B_{mn}$  and  $C_{mn}$  in (16) were determined using the initial condition (15). For this purpose, (16) was substituted into (15) and obtained:

$$\sum_{m=0}^{\infty} \sum_{n=1}^{\infty} J_m \left( \alpha_{mn} \frac{r}{R} \right) \cdot \left( B_{mn} \cos(m\phi) + C_{mn} \sin(m\phi) \right) = F(r, \phi). \tag{18}$$

The relationship (18) was successively multiplied by  $rJ_k(\alpha_{ki} r/R)\cos(k\varphi)$  and by  $rJ_k(\alpha_{ki} r/R)\sin(k\varphi)$ , and the resulting expressions were integrated with respect to the radial coordinate in the interval < 0, R > and the angular coordinate in the interval  $< 0, 2\pi >$ . As a result of these operations, and after using the orthogonality of the Bessel and trigonometric functions in the appropriate intervals, the coefficients  $B_{mn}$  and  $C_{mn}$  were obtained.

$$B_{mn} = \frac{2 \int_0^R \int_0^{2\pi} r_F(r,\phi) J_m(\alpha_{mn} \frac{r}{R}) \cos(m\phi) dr d\phi}{\pi R^2 \left(J_m^2(\alpha_{mn}) - J_{m-1}(\alpha_{mn}) J_{m+1}(\alpha_{mn})\right)},$$
(19)

$$B_{0n} = \frac{\int_0^R \int_0^{2\pi} rF(r,\phi) J_m(\alpha_{0n} \frac{r}{R}) dr d\phi}{\pi R^2 \left(J_0^2(\alpha_{0n}) + J_1^2(\alpha_{0n})\right)},$$
(20)

$$C_{mn} = \frac{2\int_0^R \int_0^{2\pi} r F(r,\phi) J_m \left(\alpha_{mn} \frac{r}{R}\right) \sin(m\phi) dr d\phi}{\pi R^2 \left(J_m^2 (\alpha_{mn}) - J_{m-1}(\alpha_{mn}) J_{m+1}(\alpha_{mn})\right)}.$$
 (21)

The coefficient  $B_{0n}$  in (20) was determined separately. Its value is two times smaller than  $B_{mn}$  for m=0. In the following analysis, the separate notation for this component was omitted, showing only the corresponding modification at m=0. In the next step of the solution, the variables under the integrals in (19)–(21) were changed, i.e.,  $r \to \rho$ ,  $\varphi \to \theta$ , and then the modified (19)–(21) were substituted into the general solution (16). The obtained solution was compared with the general solution of the same problem in (13)–(15) and expressed using the Green's function. This solution depends only on the initial condition  $F(r, \varphi)$  and has a similar form to (12) [28]. Finally, after appropriate comparison of the solutions under the integrals and also taking into account that  $t \to t-\eta$  [28], the desired Green's function was obtained.

$$G(r,\phi,t;\rho,\theta,\eta) = \frac{2}{\pi R^2} \sum_{m=0}^{\square} \sum_{n=1}^{\square} \frac{J_m(\alpha_{mn}\frac{r}{R}) \cdot J_m(\alpha_{mn}\frac{\rho}{R})}{J_m^2(\alpha_{mn}) - J_{m-1}(\alpha_{mn}) J_{m+1}(\alpha_{mn})} \cos[m(\phi-\theta)] e^{-\alpha_{mn}^2 \frac{\chi}{R^2}(t-\eta)},$$
(22)

for 
$$0 \le r, \rho \le R, 0 \le \varphi, \theta \le 2\pi, t \ge \eta$$
,

where, for the component m = 0, the right-hand side of Eq. (22) should be divided by 2.

# 4. Unsteady thermal field of conductors and their thermal parameters

The unsteady thermal field of the conductors was determined based on Eq. (12). For this purpose, Green's functions (22) were substituted into (12). After taking into account the definition of the increment (1) and analytically calculating the integral with respect to time, the unsteady temperature distributions in the conductors were obtained.

$$T_{i}(r,\phi,t) = T_{0} + \frac{2}{\pi\lambda} \sum_{m=0}^{\infty} \sum_{n=1}^{\infty} \int_{0}^{R} \int_{0}^{2\pi} D_{mni}(\rho,\theta) \left(1 - e^{-\alpha_{mn}^{2} \frac{\chi^{2} t}{R^{2}}}\right) \rho d\rho d\theta,$$

$$for \quad 0 \le r \le R, \quad 0 \le \varphi \le 2\pi, \quad t > 0, \quad i = 1, 2.$$
(23)

where

for 
$$0 \le r \le R$$
,  $0 \le \varphi \le 2\pi$ ,  $t > 0$ ,  $i = 1, 2$ ,
$$D_{mni}(\rho, \theta) = \frac{J_m(\alpha_{mn} \frac{r}{R}) J_m(\alpha_{mn} \frac{\rho}{R}) g_i(\rho, \theta) \cos[m(\phi - \theta)]}{\alpha_{mn}^2 (J_m^2(\alpha_{mn}) - J_{m-1}(\alpha_{mn}) J_{m+1}(\alpha_{mn}))},$$
(24)

and  $g_i(\rho,\theta)$  was determined using the relationship (3), after replacing  $\rho \to r$ ,  $\theta \to \varphi$ , and the right side of (23) for m=0 should be divided by 2. Due to the complicated form of the heat sources  $g_i(r,\varphi)$  (which include modules of current density), an analytical calculation of the integrals in Eq. (23) is practically impossible.

From Eq. (23) given above, for  $t \to \infty$ , it was possible to obtain the stationary temperature distributions in the conductors which, among other things, were useful in calculating the steady-state current rating.

$$T_{i}(r,\phi) = T_{0} + \frac{2}{\pi\lambda} \sum_{m=0}^{\infty} \sum_{n=1}^{\infty} \int_{0}^{R} \int_{0}^{2\pi} D_{mni}(\rho,\theta) \rho d\rho d\theta,$$

$$\text{for } 0 \le r \le R, \ 0 \le \varphi \le 2\pi, \quad i = 1, 2,$$

$$(25)$$

where for the term m = 0, the previously mentioned modification should be considered.

An important thermal parameter of conductors that determines the dynamics of the thermal field is the thermal time constant. It enables, among other things, the estimation of the duration of the transient state. In order to determine it, the well-known criterion of the averaged time constant was used [29, 30].

$$\tau_{i}(r,\phi) = \int_{0}^{\infty} \frac{T_{i}(r,\phi,t) - T_{i}(r,\phi,t\to\infty)}{T_{i}(r,\phi,t=0) - T_{i}(r,\phi,t\to\infty)} dt,$$
for  $0 \le r \le R$ ,  $0 \le \varphi \le 2\pi$ ,  $i = 1, 2$ .

After substituting (23) into Eq. (26), calculating the integral with respect to time and after appropriate simplification, the thermal time constants of the conductors were obtained.

$$\tau_{i}(r,\phi) = \frac{R^{2}}{\chi} \frac{\sum_{m=0}^{\infty} \sum_{n=1}^{\infty} \int_{0}^{R} \int_{0}^{2\pi} \frac{D_{mni}(r,\phi)}{\alpha_{mn}^{2}} \rho d\rho d\theta}{\sum_{m=0}^{\infty} \sum_{n=1}^{\infty} \int_{0}^{R} \int_{0}^{2\pi} D_{mni}(r,\phi) \rho d\rho d\theta},$$

$$\text{for } 0 \le r \le R, \quad 0 \le \varphi \le 2\pi,$$

$$(27)$$

and for m = 0 the appropriate modification should be applied.

## 5. Computational examples

Thermal field distributions (including eigenvalues) and thermal parameters were calculated using Mathematica software [31]. As a computational example, a system of two identical copper conductors with opposing current flow directions was considered. The following data were assumed:

$$R = 0.009772 \text{ m}, \ \lambda = \frac{_{360 \text{ W}}}{_{\text{mK}}}, \ I_1 = I_2 = 532.65 \text{ A}, \ T_0 = 20 ^{\circ}\text{C},$$
 
$$\gamma = 5.28262 \cdot \frac{_{107 \text{ S}}}{_{\text{m}}}, \ c = \frac{_{400 \text{ J}}}{_{\text{kgK}}}, \ \delta = 8700 \text{ kg/m3},$$
 
$$f = 50 \text{ Hz}, \ \mu_0 = 4\pi \cdot 10 - 7 \text{ H/m}, \ h = 6 \text{ W/m2K}, \ d = 0.05 \text{ m}.$$
 (28)

The calculated results of the unsteady thermal field in the conductors and the appropriate parameters are presented graphically. Figure 2 shows two-dimensional field distributions in both conductors at the times: t = 1000 s, t = 2000 s, t = 3000 s and  $t \to \infty$  (steady state). Figure 3 shows the heating curves obtained from Eq. (23) on the perimeter of the conductor at  $\varphi = \pi/2$ , located on the left side of Fig. 1. In addition, for comparison purposes, the heating curve with respect to direct current, i.e., without taking into account the skin and proximity effect, was also plotted in Fig. 3. The discussed heating curve was also obtained from Eq. (23), in which the efficiency of the heat sources (3) was defined as  $g_o = I_0/\pi R^2$  (where the direct current  $I_0$  was assumed to be equal to the rms value of the AC current given in the data set (28)). An important aspect is the discussion of the impact of the heat transfer coefficient on the thermal field distribution. Its value is generally difficult to estimate due to the varying cooling conditions and arrangement of the conductor. Therefore, Figure 4 presents the heating curves for the same conductor (and the same point as above), but for the different heat transfer coefficients. The aforementioned heating curves were plotted using the same current load, given in the data set (28). Subsequently, the thermal time constants of the conductors were determined using Eq. (27). Due to the high thermal conductivity of copper, the time constants practically do not depend on the geometric coordinates and are the same for both conductors. For the data set (28), the thermal constant is  $\tau(r, \varphi) \approx \tau = 2834$  s. Additionally, calculations showed that the thermal time constants are independent of the heat sources  $g_i(r,\varphi)$  and have the same values for both direct and alternating current loading of the conductors. However, the thermal time constant significantly depends on the cooling conditions (i.e., the heat transfer coefficient). Therefore, Fig. 5 illustrates its dependence as a function of the heat transfer coefficient on the conductor perimeter for  $\varphi = \pi/2$ , located on the left side of Fig. 1.

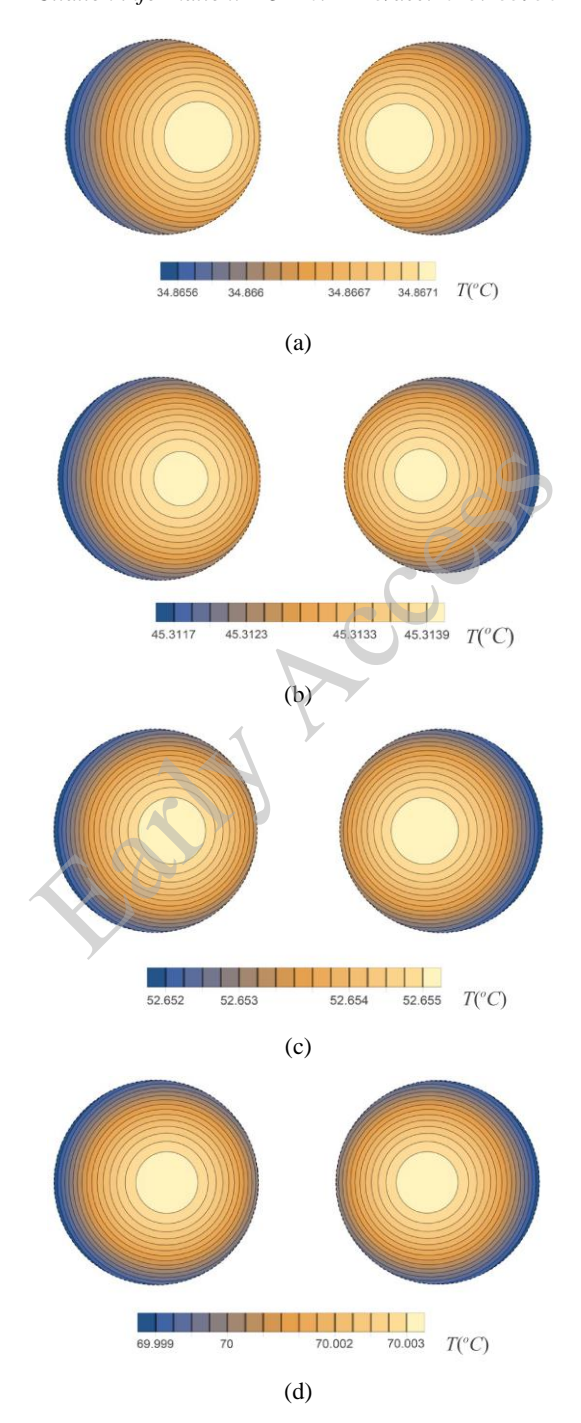


Fig. 2. Temperature field distributions in the conductors at times: (a) t = 1000 s; (b) t = 2000 s; (c) t = 3000 s; (d)  $t \rightarrow \infty$  (steady state)

In order to verify the correctness of the developed formulas (23) for I = 1, 2 describing the transient thermal field in the conductors, the boundary-initial value problem (1)–(7) was solved again. This was carried out using the finite element method (FEM) [32]. The analytical approach developed in this paper and the FEM represent completely different solution methods. In the FEM analysis, the COMSOL Multiphysics software [33] was used. The discrepancy between the results was evaluated using the following relationship:

$$\delta(r,\phi,t) = T_A(r,\phi,t) - T_N(r,\phi,t), \tag{29}$$

where  $T_A(r,\varphi,t)$  is the temperature distribution obtained using the analytical method (calculated in Mathematica program), and  $T_N(r,\varphi,t)$  is the temperature distribution obtained using the finite element method. Figure 6 shows the relation (29) at the perimeter of the conductor for  $\varphi = \pi/2$ , located on the left side of Fig. 1. At other points of both conductors, the differences (29) are almost identical to those shown in Fig. 6. Moreover, both methods yield two-dimensional field distributions of identical shapes.

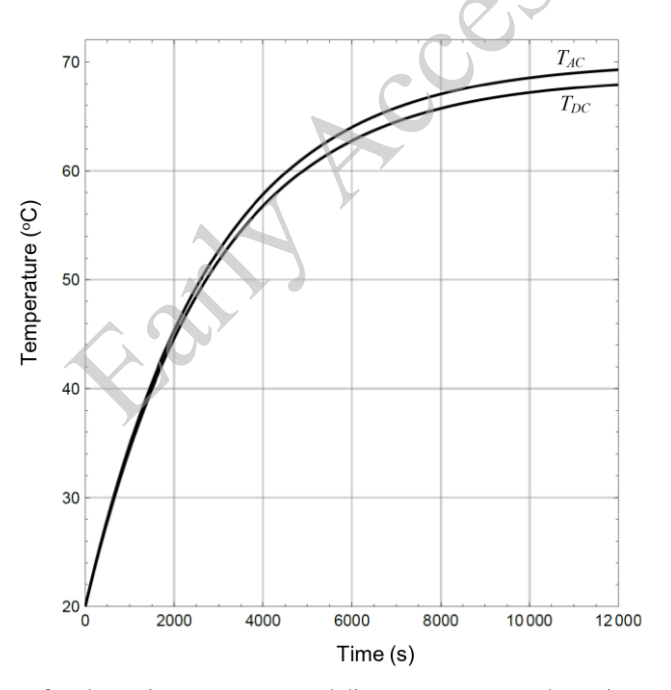


Fig. 3. Heating curves for alternating current  $T_{AC}$  and direct current  $T_{DC}$  at the perimeter of conductor 2, at the point  $\varphi = \pi/2$ , with current  $I_1 = I_2 = 532.65$  A

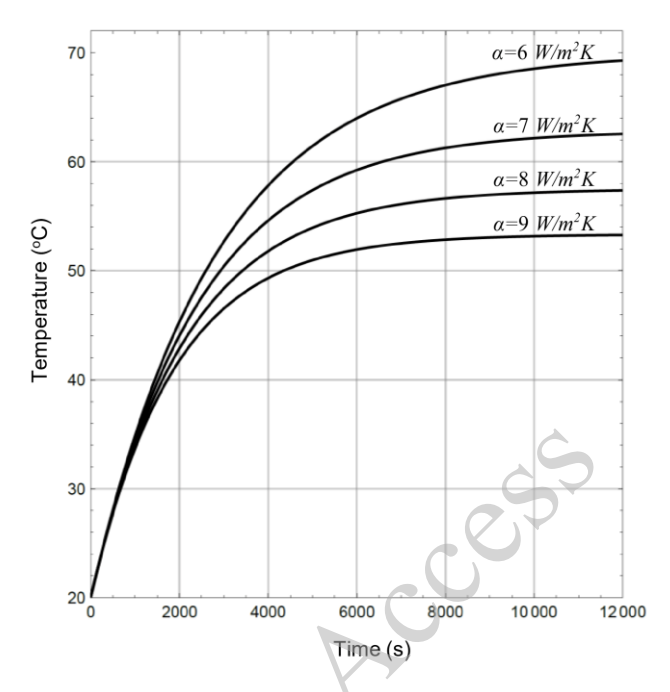


Fig. 4. Heating curves at the perimeter of conductor 2 at  $\varphi = \pi/2$ , for selected values of the heat transfer coefficient, with current  $I_1 = I_2 = 532.65$  A

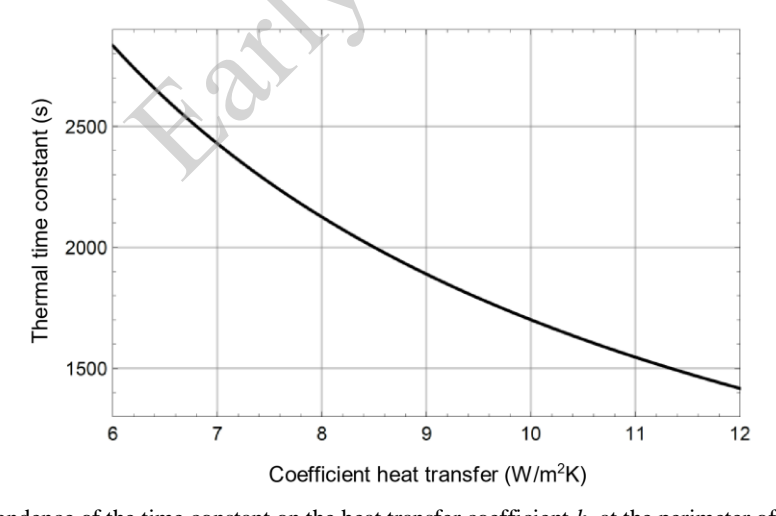


Fig. 5. Dependence of the time constant on the heat transfer coefficient h, at the perimeter of conductor 2 at  $\varphi = \pi/2$ 

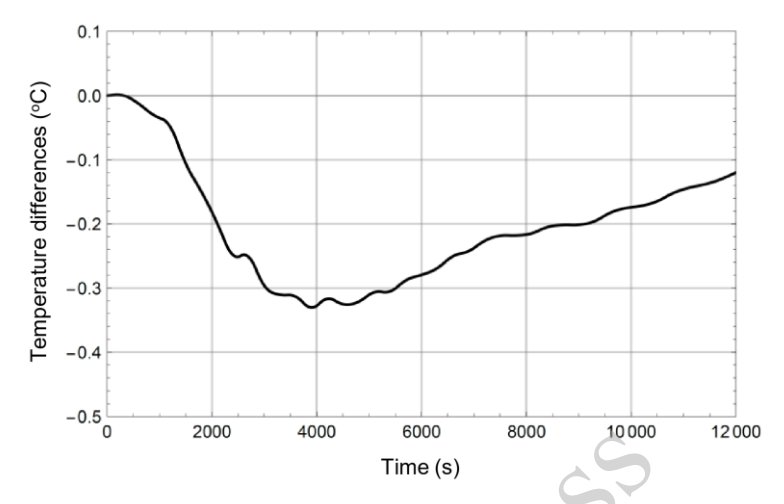


Fig. 6. Temperature differences (29) at the perimeter of conductor 2 at  $\varphi = \pi/2$  between the results obtained using the analytical method developed in the article and the finite element method (FEM)

# 6. Conclusions

This article examines the transient thermal field in a system of two parallel conductors, taking into account the skin and proximity effects. On the basis of analysis, the following conclusions can be drawn:

– The analysis of the two-dimensional temperature distributions in the conductors Figs. 2(a)–(d) shows that the temperature distributions are symmetrical with respect to the vertical axis between the conductors. This symmetry holds for identical current loading, regardless of whether the current flows in the same or opposite directions. All of the above figures show that the temperature maxima in the conductors are shifted from the center of the conductors towards their outer surfaces. Furthermore, from Figs. 2(a)–(d) it can be observed that, as time increases, the temperature maximum in the conductors shifts more towards their center. The reason for this is the uneven distribution of current density (4)–(5) resulting from the proximity and skin effect, as well as the influence of the boundary condition. The small temperature differences observed in Figs. 2(a)–(d) are caused by the high thermal conductivity of copper.

– Considering the influence of the skin and proximity effects, the heating curve for alternating current rises to a higher temperature than that for direct current (Fig. 3). At the end of the unsteady state (t = 12000 s), the temperature difference between the heating curves mentioned above is approximately 1.38°C. This is physically due to the higher electrical resistance of the conductor for alternating current, which leads to increased heat generation and consequently to a higher temperature of the conductor. Since the thermal time constant is independent of heat sources, both heating curves are characterized by the same rate of increase.

- Changes in the heat transfer coefficient significantly affect the thermal parameters of the conductors (Fig. 4 and Fig. 5). An increase in this coefficient, for example, due to improved cooling conditions, results in a lower conductor temperature (Fig. 4) and simultaneously shortens the duration of the transient state (Fig. 5).
- The thermal time constant of the conductors is independent of the heat sources (forcing). This conclusion is also confirmed by the electrical time constants of the RC and RL circuits, in which the time constants also do not depend on the excitation. In the analyzed system, using data set (28), the estimated duration of the transient state can be approximated as  $4\tau \approx 11\,336$  s. Determining this duration is particularly important in the case of intermittent and periodic operation.
- The defined temperature differences (29) between the heating curves calculated by the analytical method and the finite element method do not exceed 0.34°C. Slightly smaller discrepancies are observed at the beginning and end of the transient duration.
- In future research, the method presented in this paper will be applied to the analysis of more complex systems, such as insulated conductors. This will make it possible to investigate, among other things, the impact of the skin effect and proximity effect on a key parameter of insulated conductors their steady-state current rating. In the analysis of the above-mentioned system, it will be necessary to include additional boundary conditions related to the continuity of temperature and heat flux at the interfaces between regions.

## Acknowledgment

The paper was prepared at Bialystok University of Technology within a framework of the WZ/WE-IA/7/2023 project funded by Ministry of Education and Science, Poland

#### References

- [1] Anders G.J., Rating of electric power cables in unfavorable thermal environment, Wiley-IEEE Press (2005).
- [2] Papailiou K.O., Overhead lines, Springer (2021).
- [3] Agrawal K.C., Electrical power engineering: reference & applications handbook, Taylor & Francis (2007).
- [4] Lejdy B., Sulkowski M., *Electrical installations in building structures*, Wydawnictwo Naukowe PWN (in Polish) (2019).
- [5] Nahman J., Tanaskovic M., *Determination of the current carrying capacity of cables using the finite element method*, Electric Power Systems Research, vol. 61, no. 2, pp. 109–117 (2002), DOI: 10.1016/S0378-7796(02)00003-2.
- [6] Ghoneim S.S.M., Ahmed M., Sabiha N.A., *Transient thermal performance of power cable ascertained using finite element analysis*, Processes, vol. 9, no. 3, 438 (2021), DOI: 10.3390/pr9030438.
- [7] De Menezes E.A.W., Lisbôa T.V., Marczak R.J., A novel finite element for nonlinear static and dynamic analyses of helical cables, Engineering Structures, vol. 293, 116622 (2023), DOI: 10.1016/j.engstruct.2023.116622.
- [8] Hanna M.A., Chikhani A.Y., Salama M.M.A., Thermal analysis of power cable systems in a trench in multi-layered soil, IEEE Transactions on Power Delivery, vol. 13, no. 2, pp. 304–309 (1998), DOI: 10.1109/61.660894.

- [9] Garrido C., Otero A.F., Cidras J., Theoretical model to calculate steady-state and transient ampacity and temperature in buried cables, IEEE Transactions on Power Delivery, vol. 18, no. 3, pp. 667–678 (2003), DOI: 10.1109/TPWRD.2002.801429.
- [10] Chatzipanagiotou P., Chatziathanasiou V., Dynamic thermal analysis of a power line by simplified RC model networks: theoretical and experimental analysis, International Journal of Electrical Power and Energy Systems, vol. 106, pp. 288–293 (2019), DOI: 10.1016/j.ijepes.2018.10.009.
- [11] Mahairi M.G., Mohamed B., Arboleya P., Thermal model of DC conductors for railway traction networks: A hosting capacity assessment, Electric Power Systems Research, vol. 230, 110262 (2024), DOI: 10.1016/j.epsr.2024.110262.
- [12] Zhang Z., Deng X., Liang L., Wang X., Chen Y., Ruan J., *Temperature field calculation and thermal circuit equivalent analysis of 110 kV core cable Joint*, Processes, vol. 12, 463 (2024), DOI: 10.3390/pr12030463.
- [13] Enescu D., Colella P., Russo A., Thermal Assessment of Power Cables and Impacts on Cable Current Rating: An Overview, Energies, vol. 13, 5319 (2020), DOI: 10.3390/en13205319.
- [14] Morgan V.T., Findlay R.D., Derrah S., *New formula to calculate the skin effect in isolated tubular conductors at low frequencies*, IEE Proceedings Science, Measurement and Technology, vol. 147, no. 4, pp. 169–171 (2000), DOI: 10.1049/ip-smt:20000420.
- [15] Faria J.A.B., Raven M.S., On the success of electromagnetic analytical approaches to full time-domain formulation of skin effect phenomena, Progress In Electromagnetics Research M, vol. 31, pp. 29–43 (2013), DOI: 10.2528/PIERM13042405.
- [16] Barletta A., Zanchini E., Time averaged temperature distribution in a cylindrical resistor with alternating current, Warme Und Stoffubertragung, vol. 29, pp. 285–290 (1994), DOI: 10.1007/BF01578412.
- [17] Gołębiowski J., Zaręba M., Analytical modelling of the transient thermal field of a tubular bus in nominal rating, Compel - The International Journal for Computation and Mathematics in Electrical and Electronic Engineering, vol. 38, no. 2, pp. 642–656 (2019), DOI: 10.1108/COMPEL-02-2018-0078
- [18] Zaręba M., Gołębiowski J., *The thermal characteristics of ACCR lines as a function of wind speed an analytical approach*, Bulletin of the Polish Academy of Sciences Technical Sciences, vol. 70, no. 2, e141006 (2022), DOI: 10.24425/bpasts.2022.141006.
- [19] Gong Y., Guo X., Transient thermal analysis of power cable-considering skin effect, Proceedings of the International MultiConference of Engineers and Computer Scientists (IMECS), Hong-Kong, pp. 767–770 (2015).
- [20] Kazimierczuk M., High-frequency magnetic components, John Wiley & Sons (2013).
- [21] Wojda R.P., *Thermal analytical winding size optimization for different conductor shapes*, Archives of Electrical Engineering, vol. 64, no. 2, pp. 197–214 (2015), DOI: 10.1515/aee-2015-0017.
- [22] Arslan S., Tarimer İ., Güven M.E., Investigation of current density, magnetic flux density, and ohmic losses for single-veined, Litz and foil structured conductors at different frequencies, Pamukkale University Journal of Engineering Sciences, vol. 19, no. 3, pp. 195–200 (2013), DOI: 10.5505/pajes.2013.36844.
- [23] Latif M.J., Danesh-Yazdi A.H., Heat conduction, Springer (2024).
- [24] Wang L., Zhou X., Wei X., Heat conduction: mathematical models and analytical solutions, Springer-Verlag (2008).
- [25] Jabłoński P., Szczegielniak T., Kusiak D., Piątek Z., Analytical-numerical solution for the skin and proximity effect in two parallel round conductors, Energies, vol. 12, no. 18, 3584 (2019), DOI: 10.3390/en12183584.
- [26] Arfken G.B., Weber H.J., *Mathematical methods for physicists*, sixth edition, Elsevier Academic Press (2005).
- [27] Janicki M., De Mey G., Napieralski A., Application of Green's functions for analysis of transient thermal states in electronic circuits, Microelectronics Journal, vol. 33, pp. 733–738 (2002), DOI: 10.1016/S0026-2692(02)00057-5.
- [28] Hahn D.W., Ozisik M.N., Heat conduction, John Wiley&Sons (2012).

- [29] Sikora R., Electromagnetic field theory, Wydawnictwo Naukowo-Techniczne (in Polish) (1998).
- [30] Brykalski A., Über die eindringzeit des elektromagnetischen feldes in leiter, Archiv für Elektrotechnik, vol. 68, pp. 299–304 (1985), DOI: 10.1007/BF01845943.
- [31] Wolfram Research, Mathematica, Version 11.1. Wolfram Research Inc. (2017).
- [32] Canuto C., Quarteroni A., Zampieri T., Finite element methods for differential equation, Springer (2022).
- [33] COMSOL Multiphysics, Reference Manual, Version 5.0, COMSOL AB (2014).

